Preliminary Moho depth determination from receiver function analysis using AlpArray stations in Hungary

Dániel Kalmár[1,2], Bálint Süle[2], István Bondár[2] and the AlpArray Working Group

Dániel Kalmár
kalmardani222@gmail.com

[1] Department of Geophysics and Space Science, Institute of Geography and Earth Sciences, Eötvös Loránd University, Budapest, Hungary

[2] Kövesligethy Radó Seismological Observatory, Geodetic and Geophysical Institute, Research Centre for Astronomy and Earth Sciences, Hungarian Academy of Sciences (MTA CSFK GGI KRSZO), Budapest, Hungary

Abstract

Receiver function analysis is applied to the western part of the Pannonian Basin, a rather complex region both geologically and geodynamically. Previous receiver function analyses in this region had to deal with much smaller station density and time span than those available to us. In the analysis we used the data of some 48 seismological stations. These include not only the permanent stations from Hungary and permanent stations from neighbouring countries (Slovakia and Slovenia), but also the temporary broadband stations that were installed within the framework of the AlpArray project. Having applied rather strict manual quality control on the calculated radial receiver functions we stacked the receiver functions. Using the H-K grid search method we determined the Moho depth and the Vp/Vs ratio beneath the seismological stations in the western part of the Pannonian Basin. The unprecedented density of the AlpArray network, combined with the permanent stations, allowed us to derive high resolution Moho and Vp/Vs maps for the West Pannonian Basin, together with uncertainty estimates. Our preliminary results agree well with previous studies and complement them with finer details on the Moho topography and crustal thickness.

Keywords

Pannonian Basin; AlpArray project; Receiver function analysis; Moho discontinuity

1 Introduction

Our region of interest was the western part of the Pannonian Basin and the easternmost part of the Eastern Alps. The Pannonian Basin is a geologically complex extensional back-arc basin in Central Europe (Horváth et. al. 2006). It is characterized by compression stress fields and left strike-slip movements (Fodor 2010). The Eastern Alps has similar evolution history to the Pannonian Basin (Schmid et. al. 2008). The region shows medium seismic activity due to the advance of the Adriatic microplate. The Vienna Basin has similar sediment thickness as the Pannonian Basin but unlike the Pannonian Basin, the Mur-Mürz-Zilina zone is a seismically very active area (Horváth et. al. 2006).

The receiver function method is based on the notion that teleseismic waveforms contain information that can be used to determine the crustal and upper mantel characteristics of the Earth underneath seismic stations (Ammon 1991). In this paper, we applied receiver function analysis to determine the depth of the crust-mantle boundary under the West Pannonian Basin.

The first crustal thickness map of the Carpathian-Pannonian region was composed by Horváth (1993) by using the available national maps mostly based on reflection seismic measurements. Lenkey (1999) modified the map by making compatible the seismically obtained pattern with the gravitational anomalies of the basin. Taking into account of new deep seismic profiles and results of gravitational modelling studies Horváth et al. (2006) improved a new Moho map. The most recent version of this map is published by Horváth et al. (2015).

Receiver functions were analysed by Hetényi and Bus (2007) at four permanent stations in Hungary. In case of two stations the obtained Moho depth agreed very well with the map of Horváth et al. (2006), at the other two ones receiver function analysis indicates about 5 km thicker crust.

Grad et al. (2009) compiled the first digital, high-resolution map of Moho for the whole European Plate from individual seismic profiles, body and surface wave tomography studies, receiver function results and maps of seismic and gravity data compilations.

Recently the crustal structure of the region studied in this paper was investigated by applying ambient noise tomography by Ren et al. (2013) and by receiver functions analysis by Hetényi et al. (2015). These studies used the data of the Carpathian Basin Project array which comprised three lines of broadband seismometers and covered a 75 km wide zone across the western Pannonian Basin.

Thanks to the AlpArray project the station density and time span we could use in this study is much larger. The AlpArray project is a European initiative, with the aim to advance our understanding of orogenesis and its relationship to mantle dynamics, surface processes and seismic hazard in the Alps-Apennines-Carpathians-Dinarides orogenic system. We calculated receiver functions and determined depth of Moho beneath 13 permanent stations and 29 temporary AlpArray stations.

2 Data

The AlpArray seismic network provides uniform coverage of the greater Alpine area with seismometers deployed at unprecedented density. This presents 220 permanent and 350 temporary AlpArray seismological broadband stations (Hetényi et. al. 2018). The waveform data are available for participants of the project, at the ORFEUS EIDA node (European Integrated Data Archive). The Hungarian component of this network consists of 14 broadband stations in addition to the 9 permanent stations of the Hungarian National Seismological Network (HNSN) (Gráczer et al. 2018). The experiment has officially started on January 1, 2016. Thus, besides data from the HNSN and the Hungarian component of the AlpArray temporary deployment, we used 10-month worth of data from 15 stations of the AlpArray temporary network and 4 permanent stations from neighbouring countries (Slovakia and Slovenia). As for the HNSN broadband stations we used all available data from the start date of their operations up until October 31, 2016. Figure 1 shows the 13 permanent stations and 29 temporary AlpArray stations we used for the receiver function analysis.

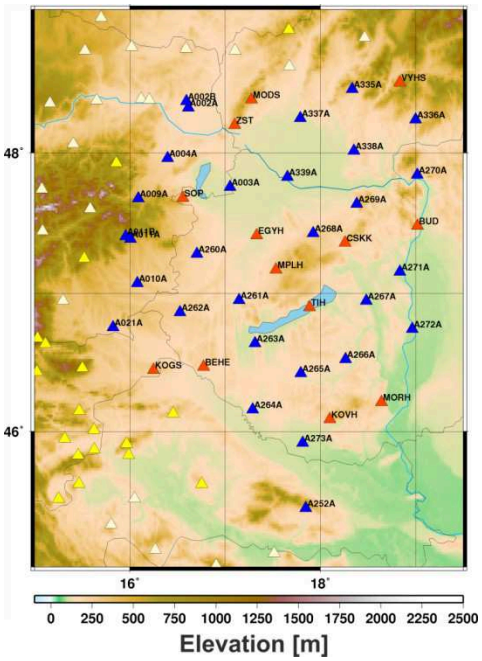

Figure 1. The map shows the seismic network in the West Pannonian Basin. The red triangles represent permanent stations and the blue triangles represent temporary AlpArray stations. The yellow and white triangles show the non-Hungarian permanent and temporary AlpArray stations that were not used in this study.

For the receiver function analysis we considered waveforms from teleseismic earthquakes between 25-96° epicentral distances and magnitudes larger than 5.5. The selection of events is expected to provide reasonable signal to noise ratio. Note that we extended the upper bound of epicentral distances from 90° to 96° so that we can get better azimuthal coverage by including events along the west coast of Central and Northern America. Figure 2a shows the selected events. Figure 2b shows the back azimuthal coverage indicating that the vast majority of earthquakes occurred in the Himalayas, the Indonesian archipelago and Japan. We downloaded the broadband three-component waveforms from the HNSN and ORFEUS-EIDA servers.

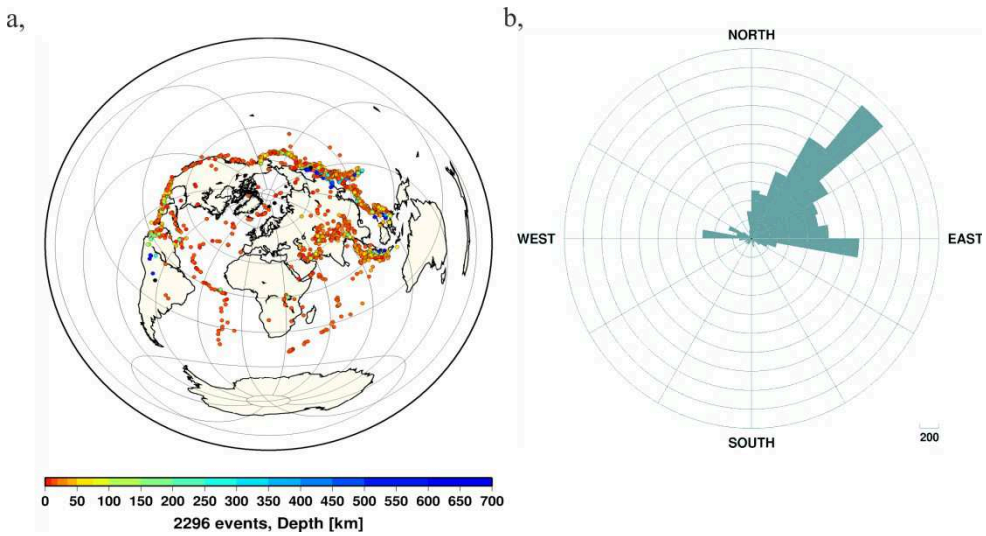

Figure 2a) The map shows the 2296 earthquakes that were used in the receiver function analysis. 2b) most of the earthquakes occurred in the Himalayas, the Indonesian archipelago and Japan.

To determine the time window of the waveforms to be downloaded we used the reported first P arrivals in the Hungarian National Seismological Bulletin (HNSB) for the Hungarian stations. At the non-Hungarian temporary AlpArray stations we did not use HNSB, because the reviewed bulletin for 2016 was not yet available. Therefore in this case we used predicted first P wave arrivals using the ak135 (Kennett et. al. 1995) travel time tables.

3 Receiver function analysis

The basis of the method is that incident P waves generated from teleseismic events are converted to S wave (Ps) and other multiples (PpPs and PpSs+PsPs) at discontinuities associated with large seismic velocity contrast such as the Moho discontinuity. We used broadband 3-~~-~~components seismograms for the P receiver function analysis. The procedure rotates the ZNE components into the ZRT coordinate system and performs the deconvolution by dividing Fourier transforms of the R and T components by the Fourier transform of the Z component. The computed receiver functions represent the relative response of the Earth structure below the stations without source and station effects. In other words, the receiver functions approximate the Green's function of the local structure beneath a seismic station (Grad and Tiira 2012). We applied the frequency-domain deconvolution method for the receiver function analysis in this study (Ammon 1997).

We used a 35 second time-window, with 5 seconds lead and 30 seconds lag times. Because the crustal thickness below the Pannonian Basin and investigated area is shallower than area of Central Alps and Carpathians, the 35 second time-window will include the major multiples from the Moho interface. In most cases this relatively short time-window contains useful signals with good signal-to-noise ratio. (Figure 3)

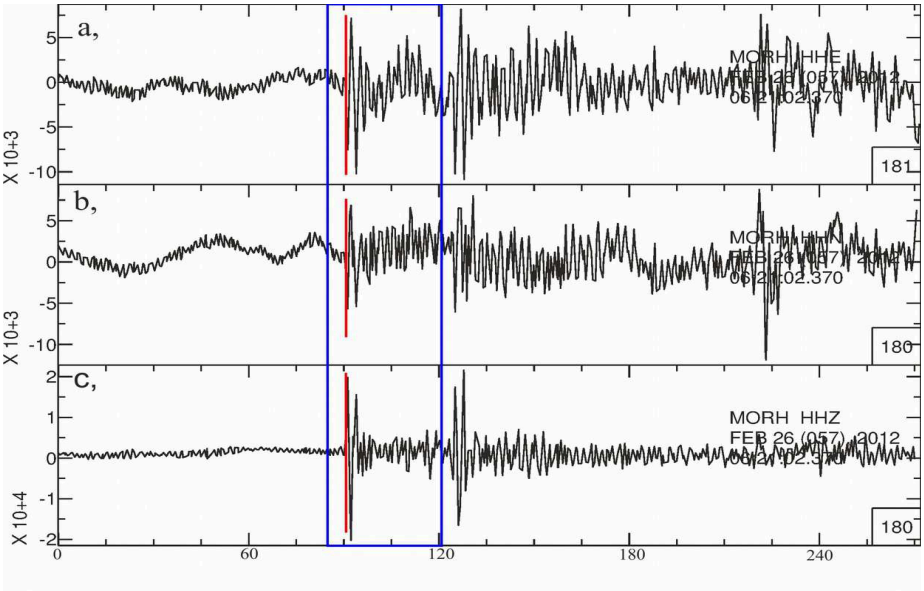

Figure 3. E, N and Z waveform components from the 2012-02-26 Taiwan earthquake recorded at MORH. The red line shows the first P arrival time. The blue lines present the start and end of a 35s time-window.

After the removal of the mean and trend, the waveforms were filtered with a Butterworth band-pass filter between 0.033 and 1 Hz (Hetényi et. al. 2015). During the pre-processing of waveforms, the Seismic Analysis Code (*SAC*, Goldstein et al. 2003), and the General Seismic

Application Computing (*GSAC*, Hermann 2013) were used. For receiver function analysis the *pwaveqn* (Ammon 1997) software is applied. The *pwaveqn* software rotates the seismograms from the ZNE system to the ZRT coordianate system and performs the deconvolution in frequency-domain. This deconvolution method strongly depends on the water-level and Gauss-filter parameters. The water-level parameter avoids division by zero by adding a small value to the denominator. The Gauss-filter removes high-frequency noise in the receiver functions, this in fact impacts the maximum amplitude of the receiver functions. The water-level and the Gaussian-filter are required parameters that were determined by trial-and-error by testing a range of values. We set the water-level and Gauss-filter values to 0.01 and 1.5, respectively. Because of the relative instability of the frequency domain deconvolution (Ammon 1997) we performed manual quality control of the radial receiver functions (Figure 4., 5.). This step represented the most time consuming process, but it was quite important to select receiver functions with the best quality. We accepted only those receiver functions where both the first-arriving P and the first multiple, Ps could be clearly seen, otherwise we rejected the receiver function. Figure 4 illustrates cases of accepted and Figure 5 shows rejected receiver functions.

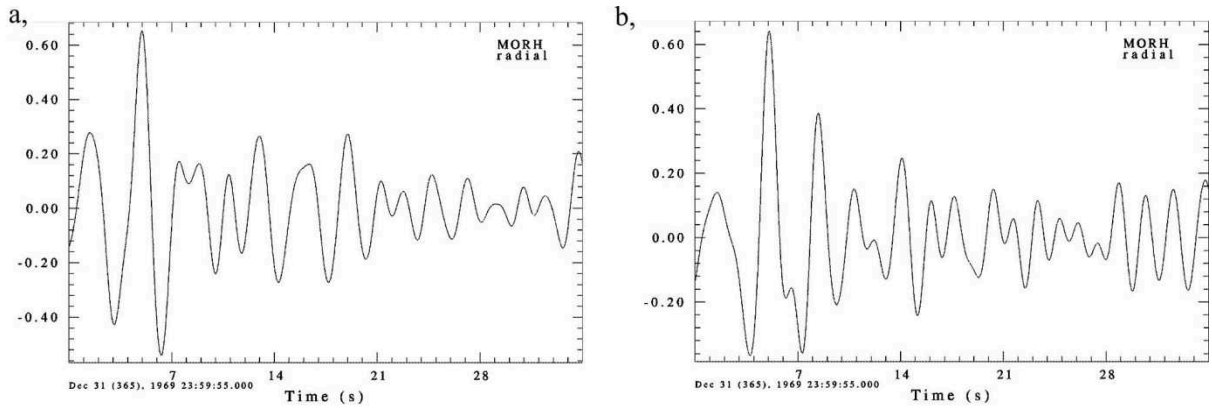

Figure 4. a) and b) acceptable receiver functions.

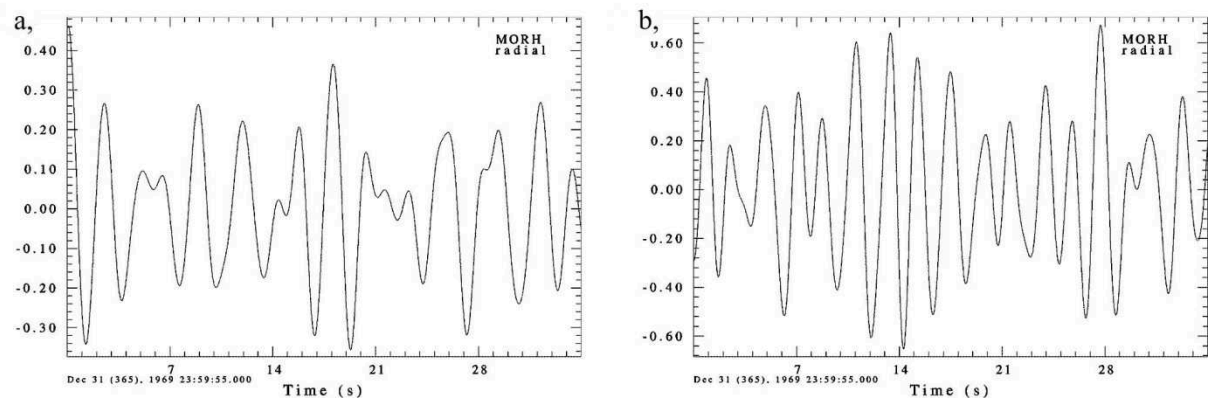

Figure 5. a) and b) the rejected receiver functions.

After the quality control process we grouped and stacked the receiver functions by back-azimuth. We grouped the receiver functions into 36, 10 degree-wide back-azimuth bins. We stacked the receiver functions in each group to increase signal-to-noise ratio for the receiver function. This grouping allowed us to investigate if there is a significant azimuthal dependence in the receiver functions. In most cases there was not, which allowed us using the full, azimuthally independent stack in our analysis. Finally, we obtained the full-stack receiver function when we stacked the receiver functions of the back-azimuth groups. Figure 6 shows an example for this stacking procedure.

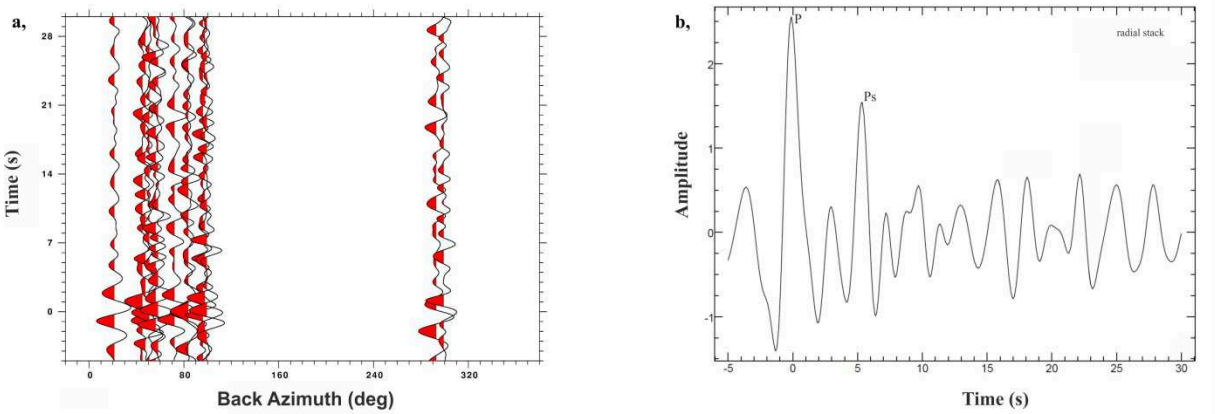

Figure 6. a) Receiver functions ordered by back-azimuth at BEHE station. b) The full-stack receiver function at BEHE.

The stacked receiver functions formed the input for the H-K grid search method (Helffrich et. al. 2013), where H represents the Moho depth and K stands for the Vp/Vs ratio. We set the Vp to 5.8 km/s, which is the average P velocity in the crust of the Pannonian Basin (Gráczer and Wéber 2012). We set the limits of H-K ~~only~~ display, the Moho depth between 20 and 40 km and for the Vp/Vs ratio between 1.5 and 2. These values represent physically meaningful limits for the Pannonian Basin. We manually checked the H-K results (Crotwell and Owens 2005) by inspecting the absolute and local maxima. We selected the physically most meaningful maximum, which was not necessarily the absolute maximum. Figure 7 shows an example of the H-K analysis at BEHE.

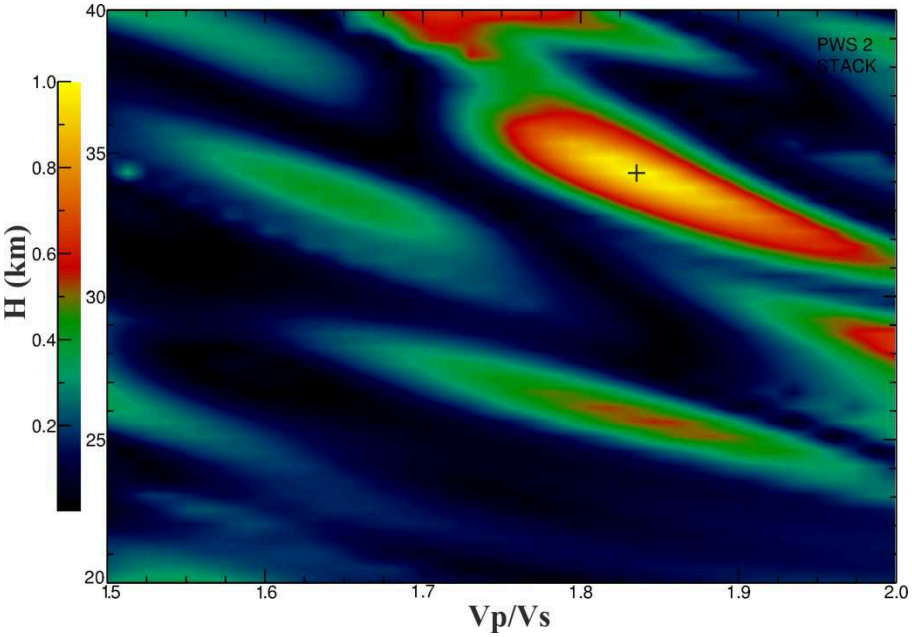

Figure 7. Results of the H-K Grid search method at the BEHE seismological station.

4 Results

We present Moho depth values and Vp/Vs ratios under the investigated stations we used in this study. Table 1 shows the results of the H-K grid search for each station.

Station code	Accepted RF.	Moho depth (km)	Vp/Vs ratio	Moho depth error (±km)	Vp/Vs ratio error (±)
BEHE	14	34.36	1.83	1.0256	0.0449
BUD	19	29.23	1.87	0.5769	0.0513
CSKK	20	29.23	1.86	2.9615	0.1385
EGYH	5	29.23	1.74	0.5128	0.0321
KOVH	9	30.77	1.78	0.8974	0.0251
MORH	29	27.51	1.71	1.9744	0.1436
MPLH	9	30.38	1.73	2.3077	0.1026
SOP	14	29.10	1.75	0.8974	0.0513
TIH	6	31.92	1.60	7.3077	0.1603
MODS	5	33.49	1.95	0.4103	0.0192
VYHS	5	33.85	1.95	0.2564	0.0205
ZST	4	25.18	1.69	0.4359	0.0224
KOGS	4	32.18	1.73	3.0769	0.1859
A260A	6	32.31	1.82	7.5000	0.1500
A261A	8	31.92	1.62	4.2308	0.2500
A262A	5	30.26	2.00	3.5678	0.2500
A263A	6	28.33	1.92	1.5385	0.1538
A264A	3	24.62	1.76	0.7692	0.1538
A265A	4	25.64	1.73	4.6154	0.1731
A266A	5	27.36	1.82	1.6667	0.1859
A267A	4	25.18	1.95	1.5256	0.1673
A268A	3	33.03	1.86	1.0897	0.1923
A269A	4	30.13	1.74	0.5128	0.0308
A270A	5	27.05	1.84	0.7692	0.0577
A271A	5	26.92	1.71	1.0256	0.0449
A272A	4	25.08	1.98	5.5000	0.1500
A273A	3	27.18	1.79	0.4615	0.1923

A335A	3	36.08	1.56	4.7949	0.1346
A336A	10	29.10	1.71	0.2179	0.2500
A337A	2	29.64	1.61	2.4359	0.1590
A338A	11	30.77	1.88	1.9231	0.0769
A339A	3	29.69	1.91	5.3077	0.2372
A002A	3	28.00	1.96	0.8333	0.1795
A002B	11	28.15	1.51	0.3590	0.0128
A003A	19	25.18	1.79	0.8718	0.0615
A004A	5	27.51	1.71	0.7179	0.0410
A009A	3	32.82	1.99	5.3846	0.0897
A010A	4	30.77	1.94	0.7692	0.0577
A011A	9	33.85	1.87	0.3846	0.0449
A011B	5	33.46	1.91	0.7692	0.0564
A021A	4	33.85	1.68	0.7692	0.0449
A252A	5	30.41	1.55	1.0897	0.0308

Table 1. The table summarizes the results. The columns present the station code, the number of accepted receiver functions, the Moho depth, the Vp/Vs ratio, the Moho-depth errors and the Vp/Vs errors.

Since the permanent stations in Hungary had longer operating periods than the rest of the stations, they produced more accepted receiver functions than the other (AlpArray and non-Hungarian permanent) stations. We only had 10-month worth of data at the AlpArray and non-Hungarian permanents stations, therefore the number of receiver functions that passed the manual review is inevitably smaller. Figure 8 shows the events with accepted receiver functions and the azimuthal coverage of receiver functions. Similar to the original distribution of the selected events shown in Figure 2, most accepted receiver functions obtained from events from the Himalayas, the Indonesian archipelago and Japan.

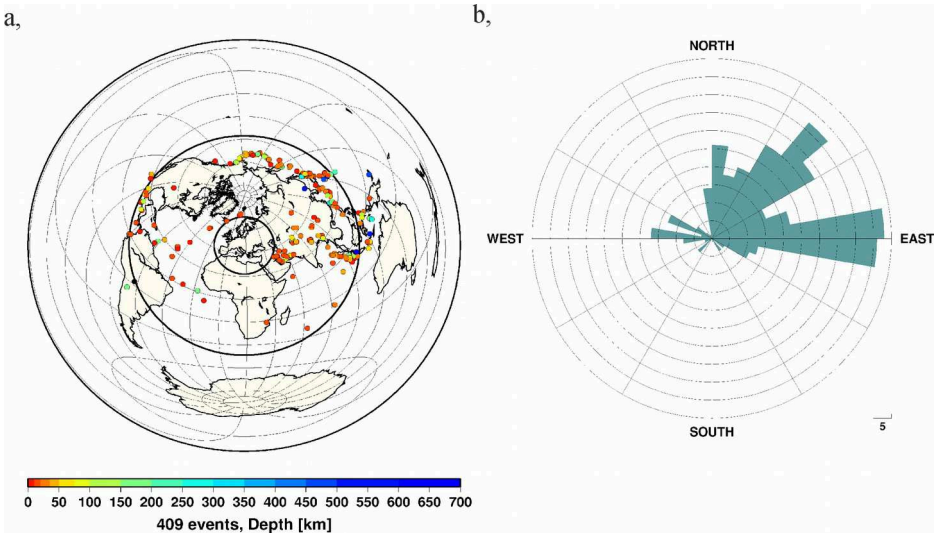

Figure 8a) The map presents the events with accepted receiver functions. 10b) back azimuthal coverage of accepted receiver functions.

Figure 9a shows the Moho map obtained from the receiver function analysis for the western part of the Pannonian Basin. We focused on the West Pannonian Basin because there we could

obtain the best resolution for the Moho map owing to the station density of the AlpArray network. Hence, we ignored the stations in the eastern part of the Pannonian. The Moho depth values change between 24 and 36 km. The Mid-Hungarian Zone and Little Hungarian Plain is characterised by thinner crust (24-28 km), while by the foothills of the Alps, Carpathians and Transdanubian Mountains indicate larger crustal thickness (31-36 km). These results are in good agreement with previous studies and complement them with finer details in the Moho topography (Grad 2009, Hetényi et. al. 2007; 2015,Lenkey 1999, Horváth 2015-).

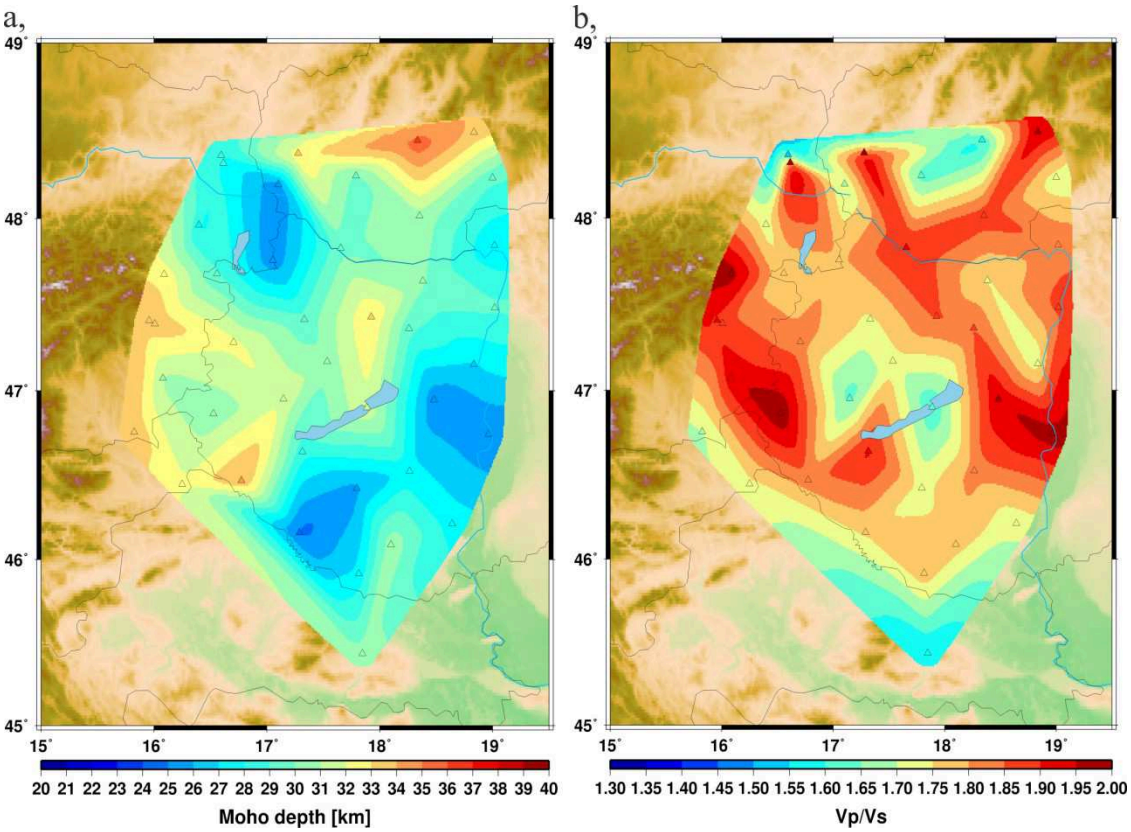

Figure 9. Maps present the Moho depth (a) and Vp/Vs ratios (b) in the western part of the Pannonian Basin from the receiver function analysis.

Figure 9b shows the Vp/Vs ratio map for the western part of the Pannonian Basin. The calculated Vp/Vs values in every case change between 1.5 and 2 in the western part of the Pannonian Basin. We obtained somewhat higher values (1.8-2) for the studied area. Recall that we used 5.8 km/s Vp velocity for every station, which is the average crustal P velocity in the Pannonian Basin (Gráczer and Wéber 2012). However, we admit that this value may not always be the best estimate in the Eastern Alps and the Carpathians. Similarly, the choice of the 35s time-window might be too short~~too short~~ for these regions. But we think both parameters are enough in the studied area.

Figure 10 shows the uncertainties in the Moho depth and Vp/Vs ratio obtained from the H-K grid search. In most cases, the Moho depth uncertainty is about one km. We obtain somewhat larger (4-7 km) values at BSZH, CSKK, TIH and A260A because the multiples were not very well defined in the full stack receiver function. The Vp/Vs ratio uncertainties vary between 0.05 and 0.25, with the majority of the errors around ±0.1.

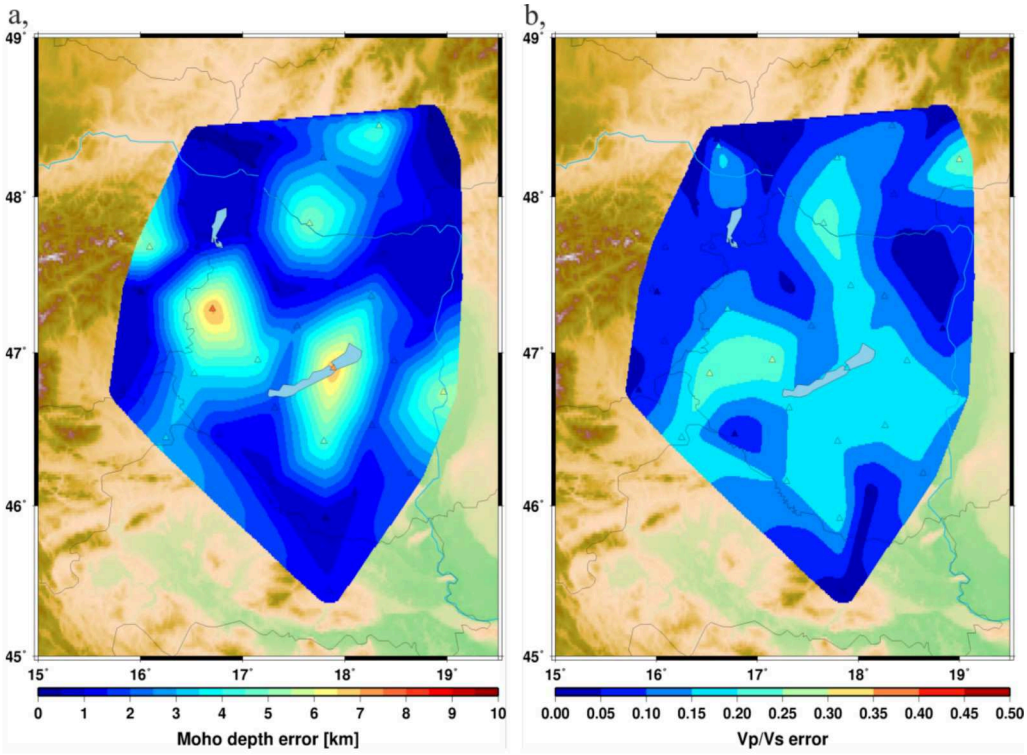

Figure 10. The maps present a) the Moho depth and b) the Vp/Vs ratio errors for western part of the Pannonian Basin obtained from the H-K analysis.

5 Discussions and Conclusions

Figure 11 show three Moho maps. First (a) is the latest published Moho map of the West Pannonian Basin (Horváth et. al. 2015), The second (b) presented by Grad (2009) from seismic profiles, body and surface wave tomography and receiver function analysis and our map. Grad presented Moho map for the whole European Plate, we cut for investigated area. The three maps are presented in the same colour scale and step interval for the sake of comparison. The comparison of the three Moho maps indicates that owing to the higher resolution provided by the AlpArray network, in most cases our results are able to resolve more subtle changes of the Moho discontinuity than the map of Horváth (2015) and Grad (2009). We can identify shallower crust (20-25 km) in the Danube~~Drava~~ Basin and in the surrounding areas, as well as in the central part of Hungary and Drava~~Danube~~ Basin on our map. Shallower zone of Danube Basin can be found map of Horváth (2015). Furthermore, the

Grad (2009) and Horváth (2015) maps show same depth ~~lightly deeper~~ values (28~~30~~-34~~35~~ km) of the crust-mantle boundary in the Transdanubian Mountains than our map~~.~~ ~~(28-34 km)~~. Our somewhat shallower Moho depth in the Transdanubian Mountains agree well with Hetényi (2015). Our map also shows deeper values below the ~~Alps and~~ Carpathians than maps of Horváth (2015) and Grad (2009). All three maps show deeper values in the Alps this thanks for the topography of the Alps.

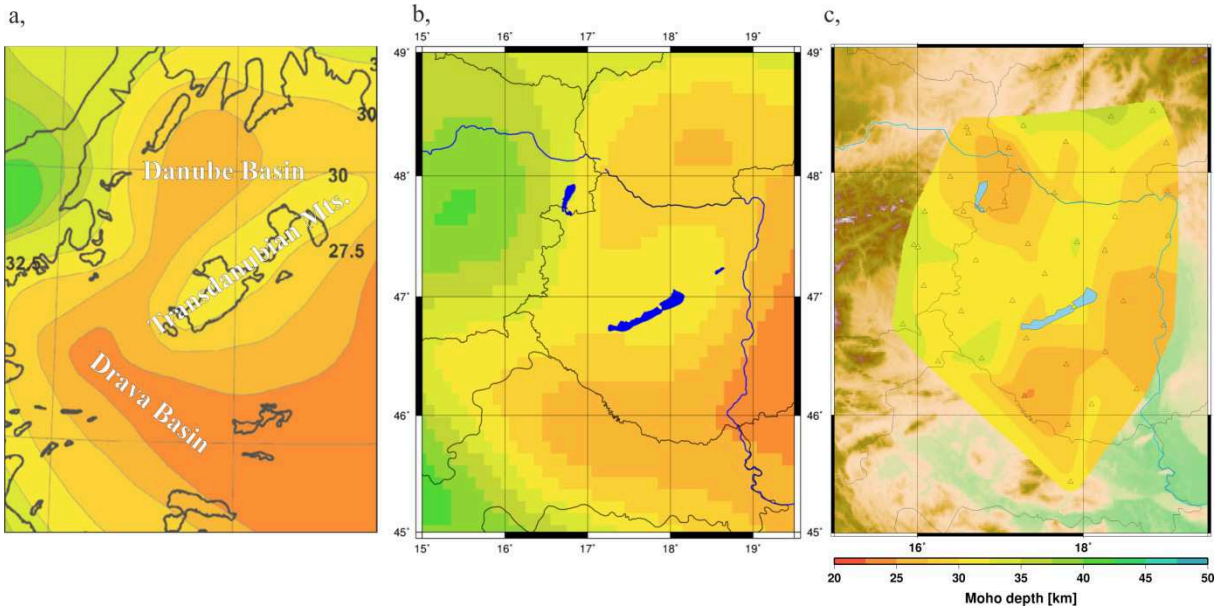

Figure 11: Comparison of the Moho maps from a) Horváth et. al. (2015), b) Grad et. al. (2009), c) from this study.

We conclude that our preliminary results, obtained purely from P-receiver function analysis, correlate well with previous studies and complement them with finer details in the Moho topography and crustal thickness. The unprecedented density of the AlpArray network, combined with the permanent stations, allowed us to derive high resolution Moho and Vp/Vs maps for the West Pannonian Basin, together with uncertainty estimates. However, during the manual quality control of the receiver functions we had to reject a large number of receiver functions because of the relative instability of the frequency domain deconvolution method. Therefore, in the follow up of this effort where we compute not only radial P receiver functions, but also S receiver functions and investigate anisotropy using both radial and transverse receiver functions, we will use the more stable, but slower iterative time-domain deconvolution (Ligorría and Ammon 1999).

Acknowledgements

The reported investigation was supported by the National Research, Development and Innovation Fund (No. K124241). Waveforms were used from the AlpArray temporary network (doi:.10.12686/alparray/z3_2015), from the Hungarian National Seismological Network (doi:10.14470/UH028726), the Slovak National Seismological Network (doi:10.14470/FX099882) as well as the Slovenian National Seismological Network (doi:10.7914/SN/SL). We would like to thank to the authors of Generic Mapping Tools (GMT) software (Wessel & Smith 1998). The authors thank the two anonymous reviewers whose comments helped to improve the paper.

References

Ammon CJ (1991) The isolation of receiver effects from teleseismic P waveforms. *Bulletin of the Seismological Society of America* 81:2504-2510.

Ammon CJ (1997) An overview of receiver function analysis.
http://eqseis.geosc.psu.edu/~cammon/HTML/RftnDocs/rftn01.html
Accessed 22.04.2017.

Crotwell HP, Owens JT (2005) Automated Receiver Function Processing. *Bulletin of the Seismological Society of America* 76:702-709.

Fodor LI (2010) Mezozoos-kainozoos feszültségmezők és törésrendszerek a Pannon-medence ÉNy-i részén – módszertan és szerkezeti elemzés. *DSc thesis*. Budapest.167 p.

Goldstein PD, Dodge M, Firpo LM (2003) SAC2000: Signal processing and analysis tools for seismologists and engineer. *The IASPEI International Handbook of Earthquake and Engineering Seismology* 1200 p.

Grad M, Tiira T, ESC Moho Working Group (2009) The Moho depth of the European

plate. *Geophysical Journal International.* 176:279–292.

Grad M, Tiira T (2012) Moho depth of the European Plate from teleseismic receiver functions. *Journal of Seismology* 16:95-105.

Gráczer Z, Bondár I, Czanik Cs, Czifra T, Győri E, Kiszely M, Mónus P, Süle B, Szanyi Gy, Tóth L, Varga P, Wesztergom V, Wéber Z (2004-2015) Hungarian National Seismological Bulletin.
http://www.seismology.hu/index.php/en/seismicity/earthquake-bulletins
Accessed 08.05.2017.

Gráczer Z, Wéber Z (2012) *One-dimensional P-wave velocity model for the territory of Hungary from local earthquake data*. *Acta Geodaetica et Geophysica Hungarica* 473:344-357.

Gráczer Z, Szanyi Gy, Bondár I, Czanik Cs, Czifra T, Győri E, Hetényi Gy, Kovács I, Molinari I, Süle B, Szűcs E, Wesztergom V, Wéber Z, AlpArray Working Group (2018) AlpArray in Hungary: temporary and permanent seismological networks in the transition zone between the Eastern Alps and the Pannonian basin. Published online to *Acta Geodaetica et Geophysica Hungarica.*

Helffrich G, Wookey J, Bastow I (2013) The Seismic Analysis Code: A Primer and User's Guide. *Cambridge University Press* 183 p.

Herrmann RB (2013) Computer programs in seismology: An evolving tool for instruction and research, *Seismological Research Letters* 84:1081-1088. doi:10.1785/0220110096

Hetényi Gy, Bus Z (2007) Shear wave velocity and crustal thickness in the Pannonian Basin from receiver function inversions at four permanent stations in Hungary. *Journal of Seismology* 11:405-414.

Hetényi Gy, Ren Y, Dando B, Stuart GW, Hegedűs E, Kovács ACs, Houseman GA (2015) Crustal structure of the Pannonian Basin: The Alcapa and Tisza Terrains and the Mid-Hungarian Zone. *Tectonophysics* 646:106-116.

Hetényi G, Molinari I, Clinton J, Bokelmann G, Bondár I, Crawford WC, Dessa JX, Doubre C, Friederich W, Fuchs F, Giardini D, Gra´czer Z, Handy MR, Herak M, Jia Y, Kissling E, Kopp H, Korn M, Margheriti L, Meier T, Mucciarelli M, Paul A, Pesaresi D, Piromallo C, Plenefisch T, Plomerová J, Ritter J, Rümpker G, Sipka V, Spallarossa D, Thomas C, Tilmann F, Wassermann J, Weber M, Wéber Z, Wesztergom V, Zivcic M, Team ASN, Crew AOC, Group AW (2018) The AlpArray Seismic Network - a large-scale European experiment to image the Alpine orogeny. Published online to *Surveys in Geophysics.*

Horváth, F. (1993) Towards a mechanical model for the formation of the Pannonian Basin. *Tectonophysics* 226:333 –357.

Horváth F, Bada G, Windhoffer G, Csontos L, Dombrádi E, Dövényi P, Fodor L, Grenercy Gy, Síkhegyi F, Szafián P, Székely B, Tímár G, Tóth L, Tóth T (2006) A Pannon-medence jelenkori geodinamikájának atlasza: Euro-konform térképsorozat és magyarázó. *Magyar Geofizika* 47:133–137.

Horváth F, Musitz B, Balázs A, Végh A, Uhrin A, Nádor A, Koroknai B, Pap N, Tóth T, Wórum G (2015) Evolution of the Pannonian basin and its geothermal resources. *Geothermics* 53:328–352

Kennett BLN, Engdahl ER, Buland R (1995) Constraints on seismic velocities in the Earth from traveltimes. *Geophysical Journal International* 122:108-124.

Lenkey L, (1999) Geothermics of the Pannonian basin and its bearing on the tectonics of basin evolution. PhD thesis. Vrije Universiteit Amsterdam 215 p.

Ligorría JP, Ammon CJ (1999) Iterative deconvolution and receiver-function estimation. *Bulletin of the Seismological Society of America* 89:1395–1400.

Ren Y, Grecu B, Stuart G, Houseman G, Hegedüs E, South Carpathian Project Working Group (2013) Crustal structures of the Carpathian-Pannonian region from ambient noise tomography. *Geophysical Journal International* 195:1351–11369. http://dx.doi.org/10.1093/gji/ggt316

Schmid SM, Bernoulli D, Fügenschuh B, Matenco LC, Schefer S, Schuster R, Tischler M, Ustaszewski K (2008) The Alpine-Carpathian-Dinaridic orogenic system: correlation and evolution of tectonic units. *Swiss Journal of Geoscience* 101:139-183.

Wessel P, Smith WHF (1998) New, improved version of the Generic Mapping Tools Released. *EOS, Transcript American Geophysical Union* 79:579.